Synthesis and Optical Properties of (Ba$_{1-x}$Sr$_x$)$_2$SiO$_2$N$_{4/3}$:Eu^{2+} Green Phosphors

Bong-Ho Kang, Jin-Ho You, Yong-Kwang Jeong, and Jun-Gill Kang[*]

Department of Chemistry, Chungnam National University, Daejeon 305-764, Korea. [*]E-mail: jgkang@cnu.ac.kr
Received May 8, 2012, Accepted October 5, 2012

Green phosphors have become very important for white light-emitting diodes (WLEDs) because of their high color rendering indices and high luminescence efficiencies.[1,2] The high thermal and chemical stabilities of Eu^{2+}-doped oxynitride green phosphors makes these species particularly interesting. Typical phosphors are MSi$_2$O$_2$N$_2$:Eu^{2+} (M = Ca, Sr and Ba), β-SiAlON:Eu^{2+}, and Sr-SiAlON:Eu^{2+}. Upon excitation in the UV-visible region, MSi$_2$O$_2$N$_2$:Eu^{2+} produced bluish-green emission for Ba^{2+} (λ$_{max}$ = 495-500 nm),[3-5] yellowish-green for Sr^{2+} (λ$_{max}$ = 540-560 nm)[2,3] and yellow emission for Ca^{2+} (λ$_{max}$ = 560 nm).[3] Similarly, Sr-SiAlON: Eu$^{2+,1}$ and β-SiAlON:Eu$^{2+,6-8}$ produced bluish-green (λ$_{max}$ = 508 nm) and yellowish-green (λ$_{max}$ = 540 nm), respectively. Tuning of the emission color for MSi$_2$O$_2$N$_2$:Eu^{2+} can be done by varying the concentration of the Eu^{2+} dopant or by replacing M^{2+} by other alkali earth ions. However, pure green emission with the peak position at 500-530 nm was not achieved with those phosphors. The present study therefore focused on the preparation and the luminescence properties of Eu^{2+}-doped M$_2$SiO$_2$N$_{4/3}$ (M = Ba and Sr) green phosphors, aiming at generating the pure green emission for use in WLEDs. The crystal structures and the luminescence properties of M$_2$SiO$_2$N$_{4/3}$-type phosphors have not been reported to now. We prepared (Ba$_{1-x}$Sr$_x$)$_2$SiO$_2$N$_{4/3}$:0.15Eu^{2+}
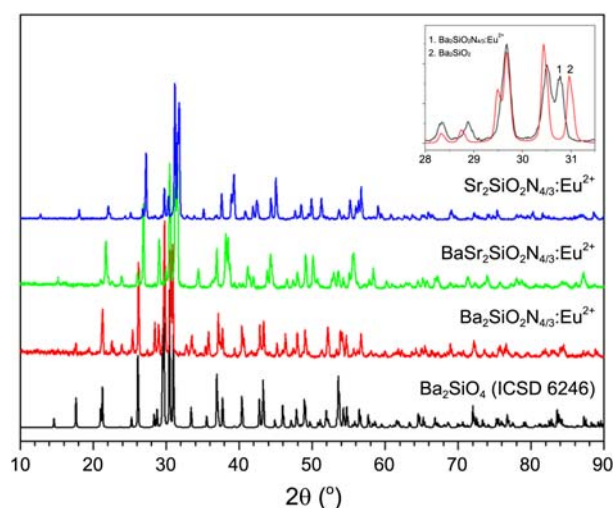
Figure 1. XRD patterns of Ba$_2$SiO$_4$ (ICSD 6246), Ba$_2$SiO$_2$N$_{4/3}$: Eu^{2+}, (Ba$_{0.5}$Sr$_{0.5}$)$_2$SiO$_2$N$_{4/3}$:Eu^{2+} and Sr$_2$SiO$_2$N$_{4/3}$:Eu^{2+}. Insert: the comparison of the main peaks of Ba$_2$SiO$_4$ (ICSD 6246) and Ba$_2$SiO$_2$N$_{4/3}$:Eu^{2+}.

phosphors and then measured their X-ray diffraction (XRD) patterns to investigate the substitution effect of Ba^{2+} by Sr^{2+} on the crystal structures. Figure 1 shows the XRD patterns of

Table 1. Crystal structural data and lattice parameters of (Ba$_{1-x}$Sr$_x$)$_2$SiO$_2$N$_{4/3}$:Eu^{2+} and M$_2$SiO$_4$ (M = Ba and Sr)

Composition	Crystal system (space group)	Lattice constants (Å)			V (Å^3)
		a	b	c	
(Ba$_{1-x}$Sr$_x$)$_2$SiO$_2$N$_{4/3}$:Eu^{2+}					
x = 0		10.1784	7.4908	5.8030	442.45
x = 0.1		10.0964	7.4531	5.7912	435.78
x = 0.2		10.0175	7.4189	5.7740	429.12
x = 0.3		9.9409	7.3845	5.7551	422.48
x = 0.4		9.8769	7.3456	5.7429	416.66
x = 0.5	Orthorhombic (Pmmm)	9.8136	7.2911	5.7200	409.28
x = 0.6		9.8023	7.2564	5.7122	406.31
x = 0.7		9.7865	7.2076	5.6910	401.42
x = 0.8		9.7682	7.1642	5.6759	397.20
x = 0.9		9.7499	7.1088	5.6676	392.82
x = 1.0		9.7271	7.0735	5.6618	385.56
Ba$_2$SiO$_4$[a]	Orthorhombic (Pmcn)	10.200	7.499	5.805	444.02
Sr$_2$SiO$_4$[b]	Orthorhombic (Pmnb)	9.773	7.090	5.682	393.71

[a]ICSD 6246. [b]ICSD 35666

$(Ba_{1-x}Sr_x)_2SiO_2N_{4/3}:Eu^{2+}$ (x = 0, 0.5 and 1). The observed XRD data of $(Ba_{1-x}Sr_x)_2SiO_2N_{4/3}:Eu^{2+}$ (x = 0 to 1) were analyzed using Fullprof 2000; the results are listed in Table 1. Crystal structures of $Ba_2SiO_2N_{4/3}:Eu^{2+}$ and $Sr_2SiO_2N_{4/3}:Eu^{2+}$ were refined as isostructural with orthorhombic Pmmm space group.

As listed in Table 1, the XRD patterns of these two oxynitride phosphors are very comparable to those of Ba_2SiO_4 (Pmcn) and α'-Sr_2SiO_4 (Pmnb), respectively. Although the ionic size of N^{3-} (1.46 Å) is larger than that of O^{2-} (1.38 Å) in the four-fold coordination, the lattice parameters of the corresponding Eu^{2+}-doped oxynitrides were slightly shortened by introducing the nitrogen atom. Consequently, the unit-cell volume was reduced from 444.02 to 442.45 Å^3 for Ba^{2+} and from 393.71 to 385.56 Å^3 for Sr^{2+}. This volume reduction is ascribed to the nature of the chemical bonds of O^{2-} and N^{3-}. The insertion in Figure 1 shows the comparison of the main peaks of $Ba_2SiO_2N_{4/3}:Eu^{2+}$ with those of Ba_2SiO_4. The partial replacement of oxygen by nitrogen resulted in the peak shift with the disappearance of the band peaking at $2\theta = 29.48°$. The bond strength of M^{2+}-N^{3-} is stronger than M^{2+}-O^{2-}, because N^{3-} has a higher formal charge, and the nephelauxetic effect is more significant compared with O^{2-}. The stronger bond strength is reflected by a shorter bond length. As listed in Table 1, the lattice parameters decreased with increasing mole fraction of Sr^{2+}. This trend is due to the smaller radius of Sr^{2+} (1.26 Å for eight-fold coordination) compared with that of Ba^{2+} (1.42 Å for eight-fold coordination). Figure 2 shows the substitution effect of Ba^{2+} by Sr^{2+} on the unit-cell volume. The linear dependence of the unit-cell volume on the mole fraction of Sr^{2+} (x) followed by Vegard's law, which was obtained by linear fitting as V/Å^3 = 439.6-53.14x (R = 0.993 and σ = 2.168) for $(Ba_{1-x}Sr_x)_2SiO_2N_{4/3}:Eu^{2+}$. The linear relationship between substituted Sr^{2+} concentration and the lattice constants suggested that the lattice constants of $(Ba_{1-x}Sr_x)_2SiO_2N_{4/3}:Eu^{2+}$ are influenced only by the relative sizes of Ba^{2+} and Sr^{2+}, i.e., $Ba_2SiO_2N_{4/3}$ and $Sr_2SiO_2N_{4/3}$ are highly miscible.

Figure 3 shows the substitution effect of Ba^{2+} by Sr^{2+} on the luminescence intensity and peak position. A significant
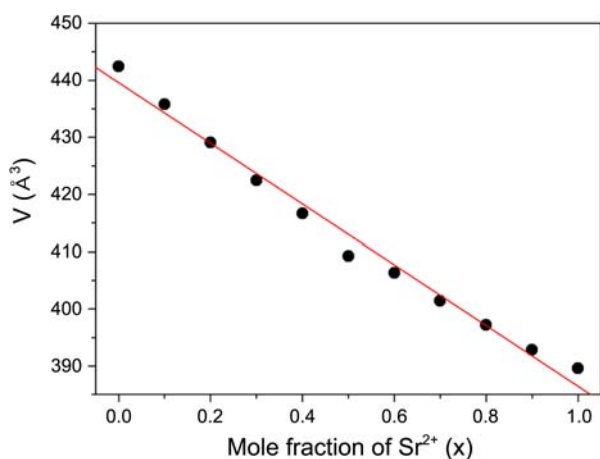
Figure 3. Effects of the replacement of Ba^{2+} by Sr^{2+} (x) in $(Ba_{1-x}Sr_x)_2$-$SiO_2N_{4/3}:Eu^{2+}$ on relative intensity (●) and peak position (○).

difference between the non-substituted and the Sr^{2+}-substituted phosphors was observed for the intensity and the peak position of the luminescence. When x = 0, i.e., the non-substituted phosphor, was excited at 460 nm, peak emission occurred at 508.5 nm. With increasing x, the intensity gradually increased and reached a maximum at x = 0.5. Above x = 0.5, the intensity rapidly decreased with increasing x, and the luminescence was almost quenched at x = 1.0. The replacement of Ba^{2+} by Sr^{2+} also affected the peak position. With increasing x in $(Ba_{1-x}Sr_x)_2SiO_2N_{4/3}:Eu^{2+}$, the peak position of the luminescence gradually red-shifted up to x = 0.5, but above x = 0.5, the red-shifting occurred rapidly. The optimal composition is $BaSrSiO_2N_{4/3}$, because this composition phosphor produced pure green emission (λ_{max} = 520 nm) with the strongest intensity. Figure 4 shows the emission and the excitation spectra of $BaSrSiO_2N_{4/3}:Eu^{2+}$. The excitation spectrum, peaking at 470 nm, was very broad with a bandwidth at half maximum of 9410 cm^{-1}. These results indicated that the blue LED is very suitable as a pumping source for the prepared green phosphor. It should be noted that $Ba_2SiO_4:Eu^{2+}$ produced the maximum intensity under 400 nm excitation.[9] We also investigated the replace-

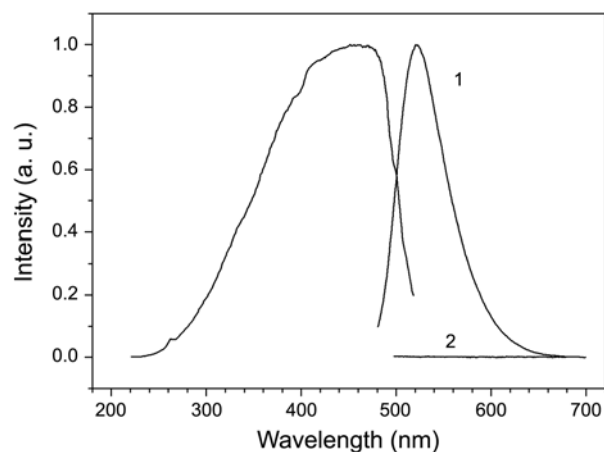**Figure 2.** Unit-cell volume versus x. The line represents the linear fitting.

Figure 4. Emission (λ_{exn} = 460 nm) and excitation (λ_{ems} = 550 nm) spectra of $BaSrSiO_2N_{4/3}:Eu^{2+}$ (1), and emission spectrum of $BaMgSiO_2N_{4/3}:Eu^{2+}$ (2).

Notes

Bull. Korean Chem. Soc. **2013**, Vol. 34, No. 1   269
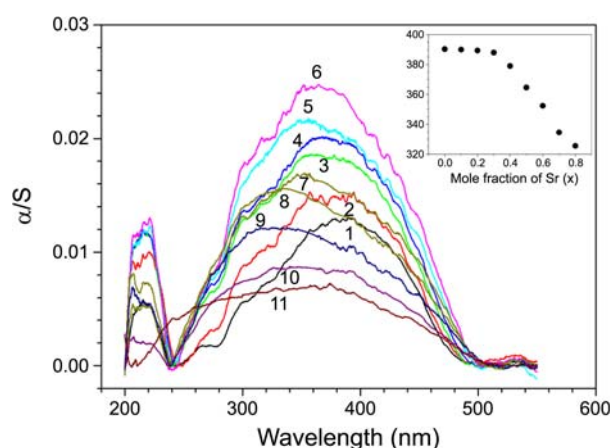
Figure 5. Diffuse reflectance spectra of $(Ba_{1-x}Sr_x)_2SiO_2N_{4/3}:Eu^{2+}$: x = 0 (1) to 1 (11) step by 0.1. Insert: the dependence of the barycenter on x.

ment effect of Ba^{2+} by Ca^{2+} and Mg^{2+} on the luminescence properties of $Ba_2SiO_2N_{4/3}:Eu^{2+}$. These two Ca^{2+} and Mg^{2+} ions, however, significantly quenched the luminescence intensity, irrespective of the level of substitution (Fig. 4). In addition, the intensity and the peak position of the phosphor was investigated as a function of the Eu^{2+} concentration. It was found that the peak position was nearly independent on the Eu^{2+} concentration, but the maximum intensity was observed in the 10-20 mol % of Eu^{2+} in $BaSrSiO_2N_{4/3}$.

We also measured the diffuse reflectance spectra of $(Ba_{1-x}Sr_x)_2SiO_2N_{4/3}:Eu^{2+}$ to investigate how the excited states of the emitting center were affected by the substitution. As shown in Figure 5, $(Ba_{1-x}Sr_x)_2SiO_2N_{4/3}:Eu^{2+}$ has a typical absorption spectrum arising from the $4f^7 \rightarrow 4f^65d$ transition of Eu^{2+}.[10] For $Ba_2SiO_2N_{4/3}:Eu^{2+}$, a strong absorption band appeared at 390 nm and a weak band at 219 nm. These two absorption bands are associated with T_{2g} and E_g states, respectively.[10] The high-energy (HE) band was very narrow and its peak position was invariant with x: $\bar{\lambda}$ = 215.3 nm (σ = 2.0). However, its intensity increased with increasing x and reached a maximum at x = 0.5. Above x = 0.5, the intensity decreased with increasing x, and disappeared when Ba^{2+} was totally replaced by Sr^{2+}. In contrast, the low-energy (LE) band was very broad and asymmetric, indicating that the excited T_{2g} state was complex. Significantly, the barycenter of the absorption band of $(Ba_{1-x}Sr_x)_2SiO_2N_{4/3}:Eu^{2+}$ was very dependent on x. As shown in the inserted figure, with increasing x, the barycenter of the LE band gradually blue-shifted up to x = 0.3, but above x = 0.3, the blue-shifting occurred rapidly. The trend of the Sr^{2+}-substitution effect on the absorbance was very similar to that on the luminescence intensity. The blue-shift of the absorption and the red-shift of the luminescence, arising from the substitution of Ba^{2+} by Sr^{2+}, are associated with the crystal-field strength surrounding Eu^{2+}.

In summary, we prepared Eu^{2+}-doped $Ba_2SiO_2N_{4/3}$ phosphor and examined the substitution effect of Ba^{2+} by other alkali earth ions on the luminescence properties. We found that only Sr^{2+} enhanced the luminescence intensity marked-

ly. We prepared $(Ba_{1-x}Sr_x)_2SiO_2N_{4/3}:Eu^{2+}$ in the whole range (x = 0 to 1.0) and investigated the substitution effects of Ba^{2+} by Sr^{2+} on the crystal structure and the luminescence properties. The partial substitution of Ba^{2+} by Sr^{2+} resulted in blue-shifting the absorption and red-shifting the emission. These phenomena are strongly associated with the crystal-field strength surrounding Eu^{2+}.

Experimental Section

The phosphor was synthesized by the conventional solid-state reaction method. Pure $BaCO_3$ (99.9%), $SrCO_3$ (99.9%), Si_3N_4 (−325 mesh), Eu_2O_3 (99.999%) and M'O (M' = Ca and Mg, 99.9%) were purchased from Aldrich and used as starting materials. There were taken in stoichiometric proportions. A mixture was thoroughly mixed in an agate mortar and then transferred into alumina crucible. The mixture was fired at 900-1000 °C, depending on the composition, for 3 h under an ammonia gas in a tube furnace.

Surface element analysis and phase information of the prepared phosphors were determined by X-ray photoelectronic spectroscopy (XPS) and powder X-ray diffraction (XRD), respectively. The XPS spectrum of the optimized phosphor was recorded on a Thermo MultiLab 2000. The XPS spectrum revealed that silicon nitride was well conserved during the solid state reaction (Figure S1 in Supporting materials). Taking into account that the sensitivity of nitrogen element was very low in the XPS analysis, the observed mole ratio of N to Si (1.1) was very close to the calculated ratio (1.33). The XRD patterns of the prepared phosphors were measured using a Shimadzu XRD-6100 analyzer with a Cu Kα radiation (λ = 1.5417 Å) and. To measure the luminescence and excitation spectra, the sample was irradiated the light from a 1000-W Xe lamp (working power, 400 W; Oriel) passing through an Oriel MS257 monochromator. The spectra were measured at 90° with an ARC 0.5-m Czerny-Turner monochromator equipped with a cooled Hamamatsu R-933-14 PM tube. For the measurement of reflectance spectra, samples with equivalent cross section were casted on pulverized $BaSO_4$. The reflectance spectra of the casted samples were recorded on an UV-3101PC (Shimadzu) spectrophotometer equipped with an integrating sphere attachment. The diffuse reflectance spectra are reproduced in the form of α/S *via* the Kubelka-Munk function:[11] $\alpha/S = (1-R)^2/2R$ (where a is the absorption coefficient, *S* is the scattering coefficient, and *R* is the reflectance).

References

1. Shioi, K.; Michiue, Y.; Hirosaki, N.; Xie, R.-J.; Takeda, T.; Matsushita, Y.; Tanaka, M.; Li, Y. Q. *J. Alloys Compd.* **2011**, *509*, 332.
2. Song, Y. H.; Park, W. J.; Yoon, D. H. *J. Phys. Chem. Solids* **2010**, *71*, 473.
3. Song, X.; He, H.; Fu, R.; Wang, D.; Zhao, X.; Pan, Z. *J. Phys. D:*

Appl. Phys. **2009**, *42*, 065409.

4. Yun, B.-G.; Horikawa, T.; Hanzawa, H.; Machida, K.-I. *J. Electro-chem. Soc.* **2010**, *157*, J364.

5. Kimura, N.; Sakuma, K.; Hirafune, S.; Asano, K.; Hirosaki, N.; Xie, R.-J.; Hirosaki, N.; Xie, R.-J. *Appl. Phys. Lett.* **2007**, *90*, 051109.

6. Hirosaki, N.; Xie, R.-J.; Kimoto, K.; Sekiguchi, T.; Yamamoto, Y.; Suehiro, T.; Mitomo, M. *Appl. Phys. Lett.* **2005**, *86*, 211905.

7. Ryu, J. H.; Park, Y.-G.; Won, H. S.; Suzuki, H.; Kim, S. H.; Yoon,

C. *J. Ceram. Soc. Jpn*. **2008**, *116*, 389.

8. Ryu, J. H.; Won, H. S.; Park, Y.-G.; Kim, S. H.; Song, W. Y.; Suzuki, H.; Yoon, C. *Appl. Phys. A* **2009**, *95*, 747.

9. Wang, M.; Zhang, X.; Hao, Z.; Ren, X.; Luo, Y.; Wang, X.; Zhang, J. *Opt. Mater.* **2010**, *32*, 1042.

10. Rubio, O. J. *J. Phys. Chem. Solids* **1991**, *52*, 101.

11. Kortüm, G. *Reflectance Spectroscopy*; Springer-Verlag: New York, 1969.